Available online at www.sciencedirect.com
SCIENCE DIRECT®
International Journal of Heat and Mass Transfer 47 (2004) 937–945
International Journal of HEAT and MASS TRANSFER
www.elsevier.com/locate/ijhmt

Theoretical and experimental investigation of microwave thawing of frozen layer using a microwave oven (effects of layered configurations and layer thickness)

P. Rattanadecho *

Department of Mechanical Engineering, Faculty of Engineering, Thammasat University (Rangsit Campus), Pathumthani, 12121 Thailand

Received 30 January 2003; received in revised form 21 August 2003

Abstract

The thawing of layered sample due to microwave energy (2.45 GHz) in oven has been investigated theoretically and experimentally. Based on a model combining of the electromagnetic field and thermal model, it is shown that the variation of layered configurations and unfrozen layer thickness changes the degree of temperature level within layered sample as well as the thawing rate. This is due to the changing of characteristics of dielectric properties of phase change materials during microwave thawing process. The simulated results are in agreement with the experimental results for the microwave thawing process.

Keywords: Microwave thawing; Layered samples; Moving boundary; Microwave oven

1. Introduction

A study of thawing process in material exposed to microwave has been studied by many researchers. Pangrle et al. [1] studied coupled electromagnetics and thermal model for the thawing process of frozen cylinders (water and NaCl) using a plane wave as opposed to a resonant cavity. They also developed a one-dimensional model for microwave thawing of cylindrical samples [2]. The first investigation of two-dimensional microwave thawing in cylinders was carried out by Zeng and Faghri [3], and their model predictions were compared with experimental data. Later, Basak and Ayyapa [4] considered the two-dimensional microwave thawing studies with fixed grid based effective heat capacity method coupled with Maxwell's equations. The primary focus of their article is to incorporate and investigate the effect of liquid convection during thawing of a pure material with microwave.

In a recent work, Ratanadecho et al. [5] performed the first analysis of a two-dimensional model based on Maxwell's equations coupled with the arbitrary moving front equation. A number of other analyses of the microwave thawing process have appeared in the literatures (Bialod et al. [6], Cleland et al. [7], Taoukis et al. [8], Decareau [9], Chamchong and Datta [10], Chamchong and Datta [11] and Basak and Ayyapa [12]).

Although the literature is replete with numerical simulations of thawing process due to microwave energy, there are few papers on the investigation of microwave thawing process of layered samples with varying layer thickness inside microwave oven. One the reason may be that the analysis of microwave thawing in layered samples is considerably more challenging due to the presence of moving boundary condition, which leads to the complex interactions of thawing front, temperature profiles and microwave energy absorbed within the layered samples.

Due to the limited amount of theoretical and experimental work on microwave thawing process, the various effects are still not fully understood and a number of critical issues remain unresolved. These effects of layered

* Tel.: +66-02-564-3001; fax: +66-02-564-3010.
E-mail address: ratphadu@engr.tu.ac.th (P. Rattanadecho).

0017-9310/$ - see front matter © 2003 Elsevier Ltd. All rights reserved.
doi:10.1016/j.ijheatmasstransfer.2003.08.019

Nomenclature

a	thermal diffusivity (m^2/s)
C_p	specific heat capacity (J/kg K)
c	light velocity (m/s)
E	electric field intensity (V/m)
f	frequency (Hz)
g	gravitational constant (m/s^2)
H	magnetic field intensity (A/m)
j	complex quantity
L	latent heat (J/kg)
P	microwave power (W)
p	pressure (Pa)
Q	microwave energy absorbed (W/m^3)
R	thawing front (m)
T	temperature (°C)
$\tan\delta$	loss tangent coefficient (–)
t	time (s)

Greek symbols

ρ	density (kg/m^3)
ε	permittivity (F/m)
λ	effective thermal conductivity (W/m K)
μ	magnetic permeability (H/m)
δ	skin depth (m)

Subscripts

0	free space
a	air
i	ice
in	input
r	relative
l	liquid water
x	coordinate

configuration, layer thickness and a complete comparison between prediction and experimental data have not been studied systematically.

This work reports a comparison of simulated results based on a one-dimensional model with experimental measurements in which the microwave operating at a frequency of 2.45 GHz is used. The effects of layered configuration, layer thickness and electric field intensity input on thawing rate are clarified in detail. Furthermore, in order to deal with the thawing front during microwave thawing process, a generalize transforming coordinate is employed in this work.

2. Analysis of microwave thawing process

2.1. The rate of volumetric heat generation due to absorption of microwave

Fig. 1 shows the physical model for microwave thawing of two layers sample. It can be seen that microwave is incident on the two layers sample where the unfrozen layer is below the frozen layer.

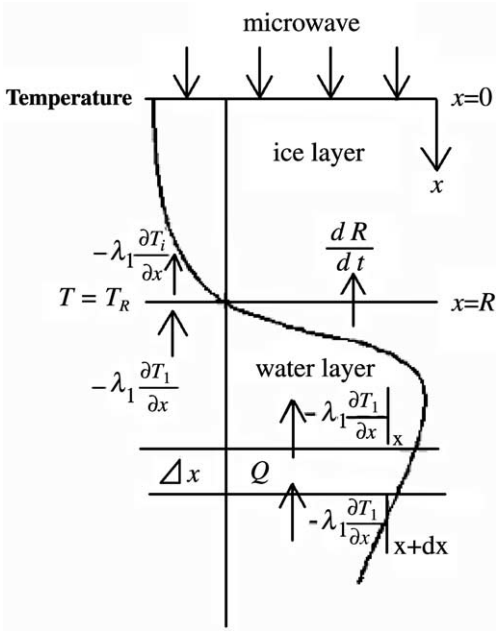

Fig. 1. Physical model.

2.1.1. Assumptions

Since the interaction between microwave energy and dielectric materials (layered samples) during microwave thawing process is a very complex phenomenon, the proposed model in present study is based on the following assumptions:

(1) The microwave field is a planar wave propagating on an infinite cylindrical test section in the microwave oven.
(2) The total amount of power absorbed within the sample subjected to microwave irradiation is constant.
(3) The values of physical properties strongly depend on temperature of sample.
(4) The effect of the sample container on the electromagnetic field can be neglected.

2.1.2. Basic equations

Generally, the relationship between the local volumetric heating rate, i.e., the density of microwave energy absorbed within the sample and the dielectric properties and electric field intensity [13] is

$$P = 2\pi f \varepsilon_0 \varepsilon_r \tan\delta E^2 \tag{1}$$

The basic equations for the electromagnetic field are based on the well-known Maxwell relations. For the microwave thawing of dielectric materials, the governing equations can be written in terms of the electric and magnetic field intensities:

$$\frac{\partial^2 E}{\partial x^2} = \sigma\mu\frac{\partial E}{\partial t} + \varepsilon\mu\frac{\partial^2 E}{\partial t^2} \tag{2}$$

$$\frac{\partial^2 H}{\partial x^2} = \sigma\mu\frac{\partial H}{\partial t} + \varepsilon\mu\frac{\partial^2 H}{\partial t^2} \tag{3}$$

where

$$E = E_0 e^{j\omega t-\gamma x}, \quad H = H_0 e^{j\omega t-\gamma x} \tag{4}$$

The propagating constant γ can be represented as a complex quantity:

$$\gamma = j\sqrt{\omega^2\mu\varepsilon - j\omega\mu\sigma} = \alpha + j\beta \tag{5}$$

where the attenuation constant α and phase constant β are related to the dielectric properties of materials:

$$\alpha = \omega\sqrt{\frac{\varepsilon\mu}{2}\left(\sqrt{\frac{\sigma^2}{\omega^2\varepsilon^2}+1}-1\right)} \tag{6}$$

$$\beta = \omega\sqrt{\frac{\varepsilon\mu}{2}\left(\sqrt{\frac{\sigma^2}{\omega^2\varepsilon^2}+1}+1\right)} \tag{7}$$

Here, the dielectric properties are strongly dependent on the temperature. Eqs. (6) and (7), it is common to use auxiliary relationships: $\tan\delta = \sigma/\omega\varepsilon$, $\varepsilon = \varepsilon_0\varepsilon_r$, $\omega = 2\pi f$ and $\mu = \mu_0$, the final form of Eqs. (6) and (7) can be rewritten respectively as [14]:

$$\alpha = 2\pi f\sqrt{\frac{\varepsilon_0\varepsilon_r\mu_0}{2}\left(\sqrt{\tan^2\delta+1}-1\right)} = \frac{2\pi f}{c}\sqrt{\frac{\varepsilon_r}{2}\left(\sqrt{\tan^2\delta+1}-1\right)} \tag{8}$$

$$\beta = 2\pi f\sqrt{\frac{\varepsilon_0\varepsilon_r\mu_0}{2}\left(\sqrt{\tan^2\delta+1}+1\right)} = \frac{2\pi f}{c}\sqrt{\frac{\varepsilon_r}{2}\left(\sqrt{\tan^2\delta+1}+1\right)} \tag{9}$$

By incorporating Eq. (5) into Eq. (4), the final form is

$$E = E_0 e^{-\alpha x}e^{j(\omega t-\beta x)}, \quad H = H_0 e^{-\alpha x}e^{j(\omega t-\beta x)} \tag{10}$$

The magnitude of the electric field decays exponentially from its value at the surface. Eq. (10), which is approximated for a infinite model as

$$E = E_{in}e^{-\alpha x} \tag{11}$$

By incorporating Eq. (11) into Eq. (1), the rate of microwave energy absorbed at any point within infinite model also varies exponentially:

$$P = 2\pi f\varepsilon\tan\delta E_{in}^2 e^{-2\alpha x} = P_{in}e^{-2\alpha x} \tag{12}$$

Furthermore, the rate of volumetric heat generation can be derived from the microwave power propagated through an infinite sample with attenuation constant, and can be written in final form as [14]:

$$Q = -\frac{\partial P}{\partial x}\,dx = 2\alpha P\,dx = 2\alpha\,dx\cdot 2\pi f\varepsilon(\tan\delta)E_{in}^2 e^{-2\alpha x} \tag{13}$$

Next, the calculation of the intensity of electric field input is required. The relationship between volumetric heat generation due to microwave energy and the local temperature rise can be expressed as a linear function:

$$Q = \rho c_p\frac{\partial T}{\partial t} \tag{14}$$

Eqs. (12) and (13) can be combined as

$$E_{in} = \sqrt{\frac{\rho c_p\Delta T}{2\pi f\varepsilon(\tan\delta)\Delta t 2\alpha\Delta x e^{-2\alpha x}}} \tag{15}$$

Eq. (15) can be used to estimate the intensity of electric field input from the measured gradient temperature, $\Delta T/\Delta t$. However, this equation is valid only in specific situations, and is not a good estimate over long time period.

2.2. Analysis of heat transport and thawing front

The temperature of the sample exposed to incident wave (Fig. 1) is obtained by solving the conventional heat transport equation with the microwave energy absorbed included as a local electromagnetic heat generation term.

2.2.1. Assumptions

In order to analyze the process of heat transport due to microwave thawing of multi-layered packed beds, the following assumptions are introduced:

(1) Like the electromagnetic field, the temperature field also can be assumed to be one-dimensional.
(2) The effect of the container on temperature field can be neglected.

(3) The effect of the natural convection in layered packed beds can be neglected.
(4) The local thermodynamic equilibrium is assumed. No chemical reactions occur in the sample.

2.2.2. Basic equations

The governing energy equation describing the temperature rise in the multi-layered packed beds are the time dependent heat diffusion equation:

$$\frac{\partial T_j}{\partial t} = a_j \frac{\partial^2 T_j}{\partial x^2} + \frac{Q_j}{\rho_j c_{pj}} \tag{16}$$

where j is layer number, a the thermal diffusivity and Q the volumetric heat generation term as defined in Eq. (13).

2.2.3. Boundary conditions

(a) Based on the physical model in Fig. 1 the moving boundary between the unfrozen layer and frozen layer is described by the Stefan equation:

$$\frac{\partial R}{\partial t} = \frac{1}{\rho_l L}\left(\lambda_l \frac{\partial T_l}{\partial x}\Big|_{x=R} - \lambda_i \frac{\partial T_i}{\partial x}\Big|_{x=R}\right) \tag{17}$$

(b) Other boundary conditions are

$$\begin{aligned} &t \geqslant 0, \quad x = 0: \ \frac{\partial T}{\partial x} = 0, \quad P = P_{in} \\ &t \geqslant 0, \quad x \to \infty: \ \frac{\partial T}{\partial x} = 0 \\ &t \leqslant 0, \quad T = T_0 \end{aligned} \tag{18}$$

3. Numerical procedure

During the solving of a moving boundary problem including phase change in microwave thawing process, complications arise due to the motion of thawing front with elapsed time. In this study, the governing equations of heat transport and moving front boundary are solved by using coordinate transformation technique based on boundary fixing method coupled with an implicit time schemes (Murray and Landis [15]).

4. Experimental apparatus

Fig. 2 shows the experimental microwave heating system. A domestic microwave oven was modified to give a steady and continuous power at a microwave frequency of 2.45 GHz, which is transmitted along the x-direction of the cylindrical test section with inner diameter of 40 mm and height of 130 mm toward a water chamber having dimensions of $150 \times 120 \times 40$ mm^3 situated at the end of the cylindrical test section. The water load ensures that only a minimal amount of microwave is reflected back to the sample.

Next we consider the sample used for testing in microwave thawing processes. The sample is composed of an unfrozen layer (water layer) and a frozen layer (ice). The unfrozen layer and the frozen layer are arranged in different configurations, as shown in state (a) and state (b), respectively. The dielectric properties of the each

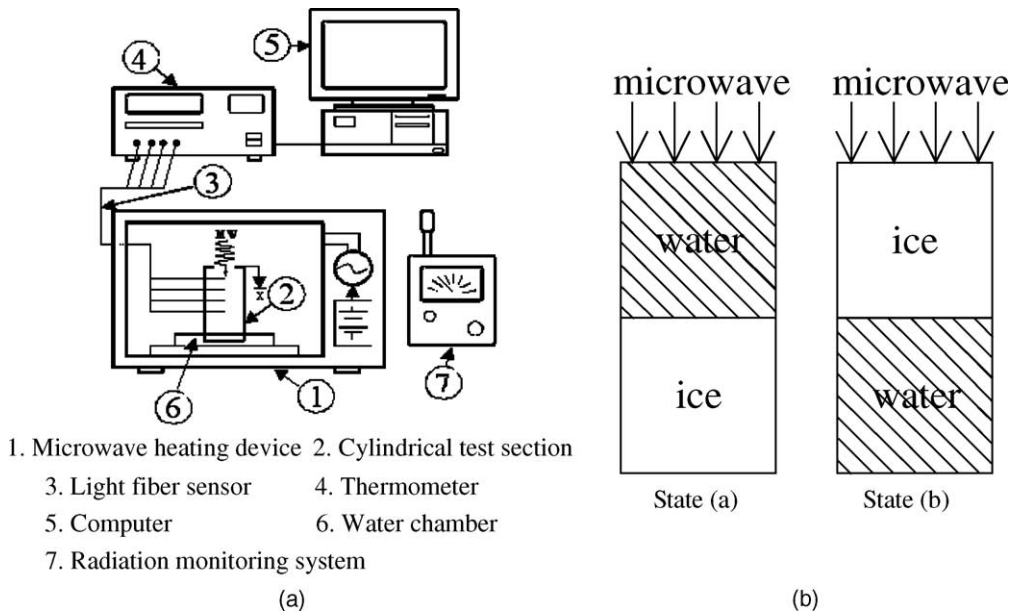

Fig. 2. Experimental apparatus: (a) microwave heating system and (b) thawing sample.

material have already been presented by Von Hippel [16].

The sample is inserted in the cylindrical test section. The aluminum foil is wrapped around the outside wall of cylindrical test section to protect any incident wave from the circumferential plane. The outside wall of aluminum foil is covered with insulation to reduce the heat loss. The temperature distributions in the sample are measured with light fiber sensors (LUXTRON Fluroptic Thermometer, Model 790, accurate to ±0.5 °C), which are placed in the center of the sample at 10 mm intervals.

During the experimental microwave thawing processes, the uncertainty of the data might come from the variations in humidity and room temperature and human errors. The uncertainty in thawing kinetics is assumed to result from uncertainty in the measured location of the thawing front. The calculated thawing kinetic uncertainties in all tests are less than 3.0%. The uncertainly in temperature is assumed to result from uncertainty in measured input power, ambient temperature and ambient humidity. The calculated uncertainty associated with temperature is less than 2.65%.

5. Result and discussion

Figs. 3–5 show the simulated and experimental results of temperature distribution within the layered sample in which (a) the unfrozen layer is above the frozen layer and (b) the unfrozen layer is under the frozen layer, corresponding to the initial temperature of 0 °C, electric field intensity input of 7000 V/m and unfrozen layer thickness of 20 mm ($xw = 20$ mm). Some of electromagnetic and thermo-physical properties used in all computations are given in Table 1 [5].

For state (a), Fig. 3 shows that the skin-depth heating effect causes a major part of incident waves to be absorbed within a thickness of about 20 mm of the leading edge of unfrozen layer. Owing to the microwave energy absorbed, the temperature distribution within the unfrozen layer decays slowly along the propagation direction.

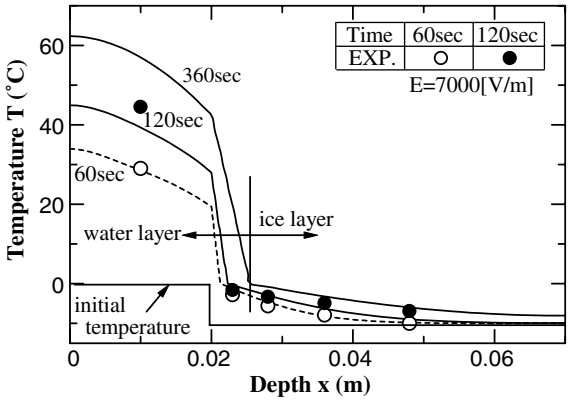

Fig. 3. Temperature profiles at various elapsed times (state (a)), $xw = 20$ cm.

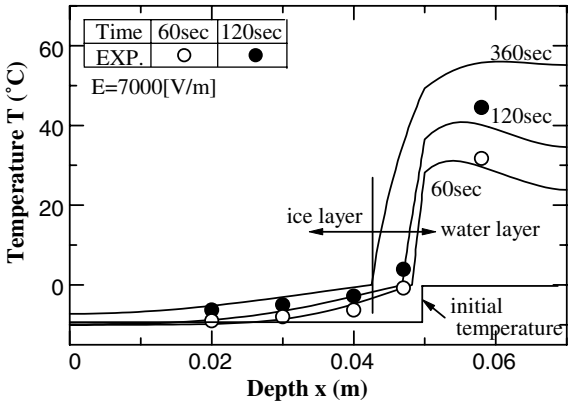

Fig. 4. Temperature profiles at various elapsed times (state (b)), $xw = 20$ mm.

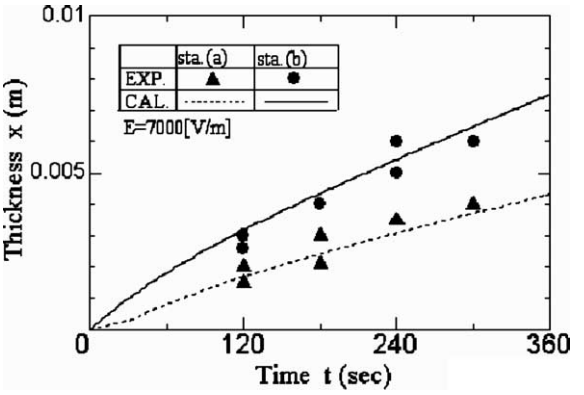

Fig. 5. Thawing thickness at various elapsed times.

Fig. 4 shows the results of state (b). The incident microwave is easily further penetrated to the unfrozen layer, which forms a highly absorptive material (higher loss tangent coefficient), since an ice in the frozen layer is a highly transparent material to microwave. The latter arises from the fact that the larger part of microwaves can be absorbed at the leading edge of the unfrozen layer. The presence of the strength of microwave energy absorbed gives rise to a hot spot at the leading edge of the unfrozen layer. This causes heat to conduct from the hotter region in unfrozen layer (higher microwave energy absorbed) to the cooler region (lower microwave energy absorbed) in the frozen layer. It is found that the upward movement of thawing front occurs at the interface between frozen layer and unfrozen layer where

Table 1
Thermal and dielectric properties of the liquid water and ice

Properties	Liquid water	Ice
ρ	1000 kg/m^3	1910.9 kg/m^3
λ	0.610 W/m K	1.48 W/m K
C_p	4.186 kJ/kg K	1.280 kJ/kg K
μ_r	1.0 H/m	1.0 H/m
ε_r	$88.15 - 0.414T + (0.131 \times 10^{-2})T^2 - (0.046 \times 10^{-4})T^3$	5.1 F/m
$\tan\delta$	$0.323 - (9.499 \times 10^{-3})T + (1.27 \times 10^{-4})T^2 - (6.13 \times 10^{-2})T^3$	0.0124

the strength of the microwave energy absorbed increases with increasing the thawing rate. As thawing progressed, the thawing rate is higher in comparison to previous case at the same time. Nevertheless, the temperature distribution within the frozen layer stays colder due to the difference between the dielectric properties of water and ice. This is because water is a highly absorptive material, while ice is highly transparent which results in a lower microwave energy absorbed within this layer. At exposure time of about 120 s, there is a difference of about 50 °C between the maximum and minimum temperatures. The simulated results are in agreement with the experimental results for microwave thawing process.

Fig. 5, which is redrawn from Figs. 3 and 4, which shows the thawing front for the cases of state (a) and state (b), respectively. In the state (a), the thawing front moves slowly with the elapsed time along the propagation direction. This is due to the fact that the most of the heat takes place at the leading edge of unfrozen layer located away from frozen layer. Consequently, a small amount of heat can conduct to the frozen layer because the water layer downstream acts as an insulator causing a slow movement of thawing front. In state (b), in contrast to that state (a), the thawing front moves rapidly with the elapsed time against the propagation direction. This is because the most of the heat directly conduct into the frozen layer due to the fact that the hot spot takes place at the leading edge of the unfrozen layer located close to the frozen layer.

The following discussion refers to the effect of the variation of unfrozen layer thickness on the heating and thawing rates during microwave thawing process, which correspond to thawing conditions shown in previous cases. Similar trends appear in Figs. 3 and 4. The heating is intense close to the leading edge of the unfrozen layer (Figs. 6–11) in all cases ($xw = 30$, 40, and 50 mm). Nevertheless, the temperature distributions rise slowly with increasing in unfrozen layer thickness due to the volumetric heating effect.

Fig. 12, redrawn from Figs. 6–11, shows the simulated results of thawing front as a parameter of unfrozen layer thickness in the cases of state (a) and state (b), respectively. Corresponding to those temperature distributions as shown in Figs. 6–11, the thawing front moves slowly with elapsed time with increasing unfrozen

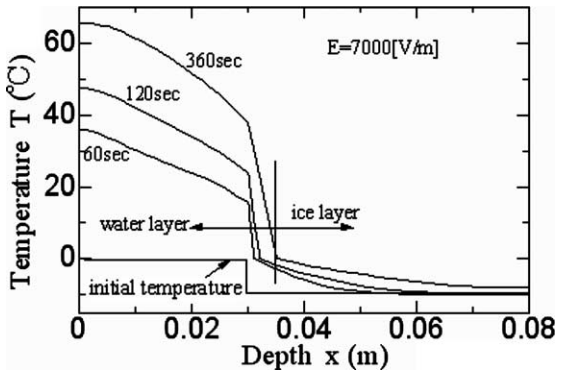

Fig. 6. Temperature profiles at various elapsed times (state (a)), $xw = 30$ mm.

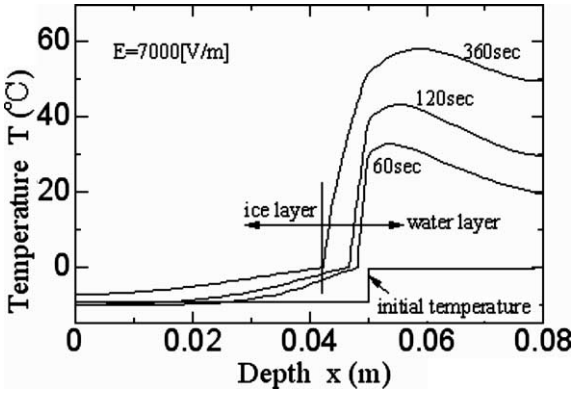

Fig. 7. Temperature profiles at various elapsed times (state (b)), $xw = 30$ mm.

layer thickness. However, the difference of the progressing of thawing front is not clearly seen in the case setting unfrozen layer under frozen layer due to heat conduction dominating thawing process.

Figs. 13–17 show the simulated temperature distributions and thawing front at various conditions when electric field intensity input is varied. It is evident from the figures that temperature and the thawing rate increase with increasing electric field intensity input.

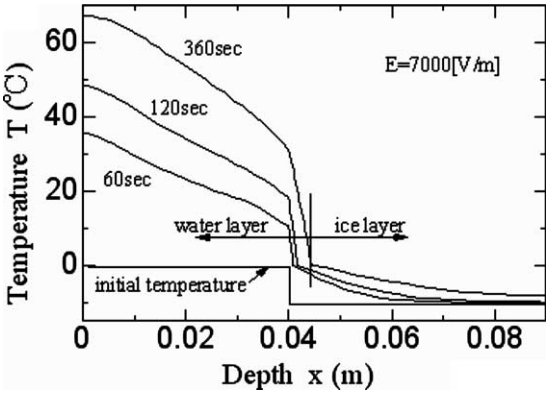

Fig. 8. Temperature profiles at various elapsed times (state (a)), $xw = 40$ mm.

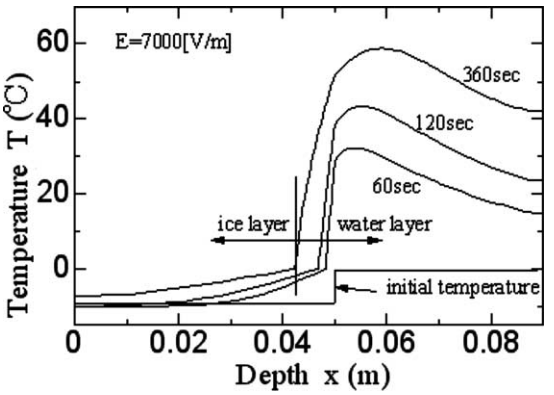

Fig. 9. Temperature profiles at various elapsed times (state (b)), $xw = 40$ mm.

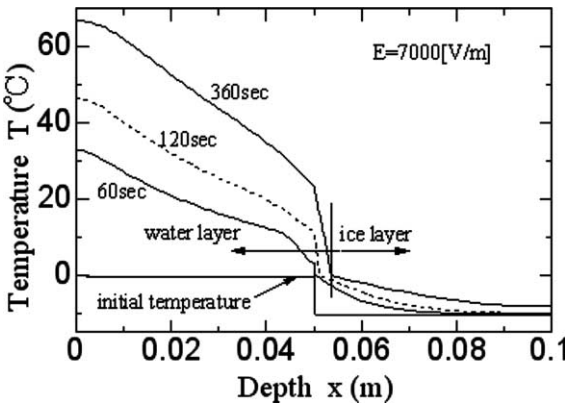

Fig. 10. Temperature profiles at various elapsed times (state (a)), $xw = 50$ mm.

Nevertheless, the observation of temperature profiles and thawing front depicted in Figs. 13–17 shows that the

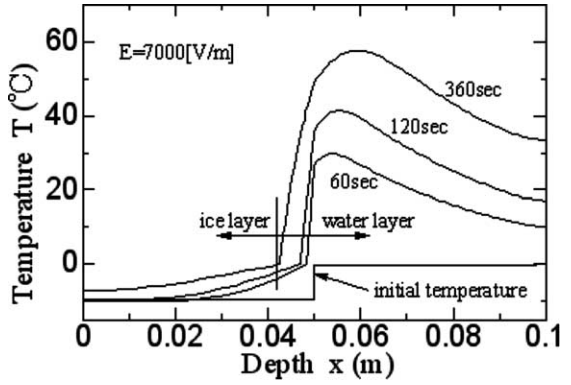

Fig. 11. Temperature profiles at various elapsed times (state (b)), $xw = 50$ mm.

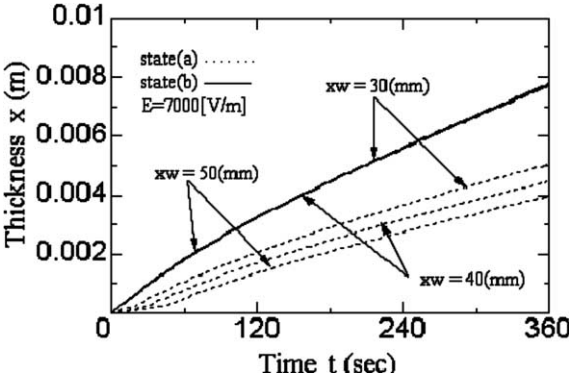

Fig. 12. Thawing thickness at various unfrozen layer thickness.

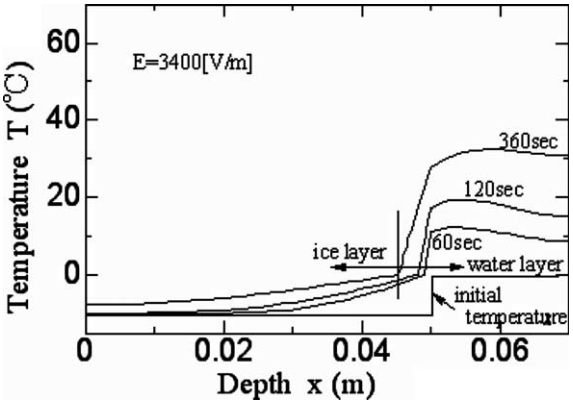

Fig. 13. Temperature profiles at various elapsed times (state (a)).

predicted results exhibit the similar trend as shown in previous cases.

In this study, the capability of the mathematical model to correctly handle the field variations at the interfaces between materials of different dielectric

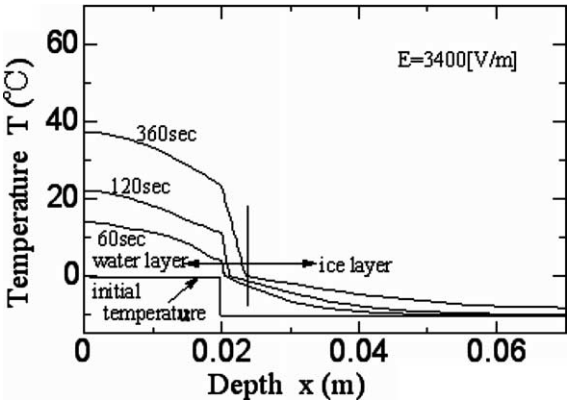

Fig. 14. Temperature profiles at various elapsed times (state (b)).

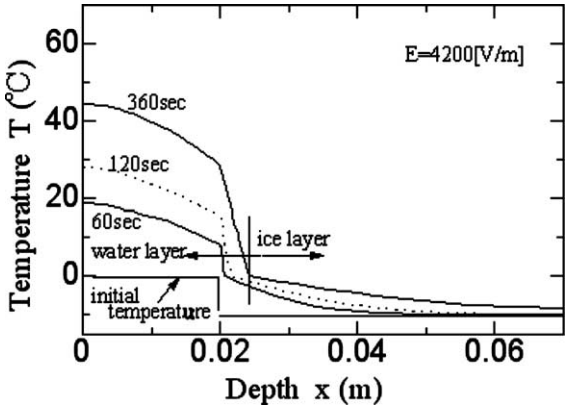

Fig. 15. Temperature profiles at various elapsed times (state (a)).

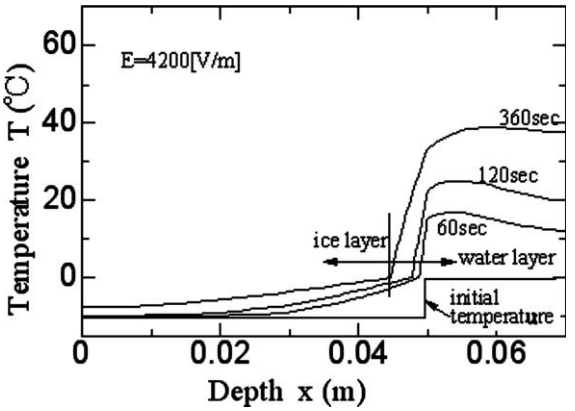

Fig. 16. Temperature profiles at various elapsed times (state (b)).

properties was shown. With further quantitative validation of the mathematical model, it is clear that the model can be used as a real tool for investigating in detail this particular microwave heating of dielectric materials at a fundamental level.

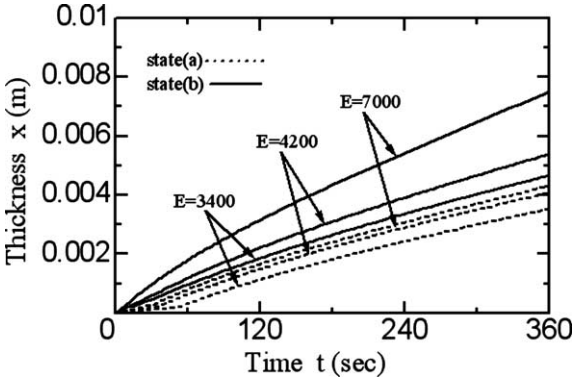

Fig. 17. Thawing thickness at various electric field intensity input.

6. Conclusion

The experiments and theoretical analysis presented in this work describe many of the important interactions within a layered sample (ice and liquid) during microwave thawing using a microwave oven. The following summarize the conclusions of this work:

(1) A generalized mathematical model of thawing using microwave oven is proposed. It is used successfully to describe the thawing phenomena under various conditions.
(2) The result shows that the changing of layered configuration changes the heating pattern within the layered sample. When the unfrozen layer is under the frozen layer (state (b)), the microwaves can penetrate further inside the unfrozen layer. The heating takes place at the leading edge of unfrozen layer and directly conducts to the frozen layer, which results in a higher thawing rate. Furthermore, the direction of thawing against the incident microwave strongly depends on the layered configuration. This is because of the differences in the dielectric properties between water and ice within layered samples.
(3) The thawing rate decreases with increasing unfrozen layer thickness.
(4) The increase in electric field intensity input leads to increase the heating rate as well as the thawing rate.

Acknowledgement

The author thanks Professor K. Aoki for some helpful discussions.

References

[1] B.J. Pangrle, K.G. Ayappa, H.T. Davis, E.A. Davis, J. Gordon, Microwave thawing of cylinders, AIChE J. 37 (1991) 1789–1800.

[2] B.J. Pangrle, K.G. Ayappa, E. Sutanto, H.T. Davis, E.A. Davis, Microwave thawing of semi-infinite slabs, Chem. Eng. Comm. 112 (1991) 39.

[3] X. Zeng, A. Faghri, Experimental and numerical study of microwave thawing heat transfer for food materials, ASME J. Heat Transfer 116 (1994) 446–455.

[4] T. Basak, K.G. Ayappa, Analysis of microwave thawing of slab with the effective heat capacity method, AIChE J. 43 (1997) 1662–1674.

[5] P. Ratanadecho, K. Aoki, M. Akahori, Characteristics of microwave melting of frozen packed bed using a rectangular wave guide, IEEE Trans. Microwave Theory Tech. 50 (6) (2002) 1487–1494.

[6] D. Bialod, M. Jolion, R. Legoff, Microwave thawing of food products using associated surface cooling, J. Microwave Power 13 (1978) 269–274.

[7] A.C. Cleland, R.L. Earl, Assessment of freezing time prediction methods, J. Food Sci. 49 (1984) 1034–1042.

[8] P. Taoukis, E.A. Davis, H.T. Davis, J. Gordon, Y. Talmon, Mathematical modeling of microwave thawing by modified isotherm migration method, J. Food Sci. 52 (1994) 455–463.

[9] R. Decareau, High frequency thawing of food, Microwave Energy Appl. Newsl. 1 (1968) 3.

[10] M. Chamchong, A.K. Datta, Thawing of food in a microwave oven I: Effect of power levels and power cycling, J. Microwave Power Electromagn. Energy 34 (1999) 9–21.

[11] M. Chamchong, A.K. Datta, Thawing of food in a microwave oven II: Effect of load geometry and dielectric properties, J. Microwave Power Electromagn. Energy 34 (1999) 22–32.

[12] T. Basak, K.G. Ayappa, Influence of internal convection during microwave thawing of cylinders, AIChE J. 47 (2001) 835–848.

[13] P. Ratanadecho, K. Aoki, M. Akahori, Experimental and numerical study of microwave drying in unsaturated porous material, Int. Comm. Heat Mass Trans. 28 (2001) 605–616.

[14] P. Ratanadecho, K. Aoki, M. Akahori, Experimental validation of a combined electromagnetic and thermal model for a microwave heating of multi-layered materials using a rectangular wave guide, ASME J. Heat Transfer 124 (6) (2002) 992–996.

[15] W.D Murray, F. Landis, Numerical and machine solutions of transient heat conduction problem involving melting or freezing, ASME J. Heat Transfer 81 (1959) 106–112.

[16] A.R. Von Hippel, Dielectric Materials and Applications, MIT Press, Boston, 1954.